AIMS Energy, 14(1): 161–184.
DOI: 10.3934/energy.2026007
Received: 01 October 2025
Revised: 17 December 2025
Accepted: 05 January 2026
Published: 22 January 2026

https://www.aimspress.com/journal/energy

Research article

Pressure driven dynamics in PEMFCs: A comprehensive study on gas pressure influence over performance efficiency and stability

Saad S. Alrwashdeh*

Mechanical Engineering Department, Faculty of Engineering, Mutah University, P.O Box 7, Al-Karak 61710 Jordan

* **Correspondence:** Email: saad.alrwashdeh@mutah.edu.jo; Tel: +962796430481.

Abstract: In this paper, we explored gas pressure as a determining factor influencing the performance, efficiency, and durability of Proton Exchange Membrane Fuel Cells (PEMFCs). An extensive simulation model was developed over operating pressures ranging from 1 to 4 atm at 353 K under fully humidified conditions. The findings indicated that increasing pressure by 1 atm to 2 atm enhances net efficiency by 17% (48.5 to 56.8%) and, correspondingly, maximum current density increases to 1.40 A cm^{-2} and the stack life is estimated to be even longer, to almost 6,000 hours. Nonetheless, beyond a pressure of 4 atm, the returns are non-linear as compressor penalties become nearly 5-fold over baseline and long-term stability decreases to 5,100 hours. These results highlight the ideal operating range of 2–3 atm, and efficiency, durability, and water balance were optimized at the same time, which is consistent with and like earlier experimental works. The article gives practical information on pressure-tuning measures of PEMFCs in vehicle, marine, and non-portable energy systems.

Keywords: efficiency-stability trade-offs; gas pressure optimization; durability enhancement; PEMFCs

Nomenclature

Symbol	Description	Unit
E	Cell potential	V
E_0	Standard reversible potential	V
R	Universal gas constant	J mol^{-1} K^{-1}
T	Temperature	K
F	Faraday constant	C mol^{-1}
p_{H2}	Partial pressure of hydrogen	atm
p_{O2}	Partial pressure of oxygen	atm
p_{H2O}	Partial pressure of water vapor	atm
V_{cell}	Cell voltage	V
η_{act}	Activation overpotential	V
η_{ohm}	Ohmic overpotential	V
η_{conc}	Concentration overpotential	V
i	Current density	A cm^{-2}

Continued on next page

Symbol	Description	Unit
i_0	Exchange current density	A cm^{-2}
α	Charge transfer coefficient	-
R_{ohm}	Area-specific ohmic resistance	Ω cm^2
i_L	Limiting current density	A cm^{-2}
n	Number of electrons	-
A_{act}	Active area per cell	cm^2
N_{cell}	Number of cells in stack	-
P_{stack}	Stack power	W
P_{BOP}	Balance-of-plant power	W
P_{net}	Net system power	W
η_{sys}	Net system efficiency	%
m_{air}	Air mass flow rate	kg s^{-1}
cp	Specific heat of air	J kg^{-1} K^{-1}
Tin	Compressor inlet temperature	K
η_{comp}	Compressor isentropic efficiency	-
γ	Heat capacity ratio of air	-
p_{out}	Compressor outlet pressure	Pa
p_{in}	Compressor inlet pressure	Pa
μ	Dynamic viscosity	Pa s
k	Permeability of porous medium	m^2
u	Superficial velocity	m s^{-1}
D_{AB}	Binary diffusion coefficient	m^2 s^{-1}
D_{eff}	Effective diffusion coefficient	m^2 s^{-1}
c_{bulk}	Bulk concentration	mol m^{-3}
c_{surf}	Surface concentration	mol m^{-3}
δ	Diffusion layer thickness	m
n_d	Electro-osmotic drag coefficient	-
J_{drag}	Water flux due to drag	mol m^{-2} s^{-1}
J_{bd}	Back-diffusion water flux	mol m^{-2} s^{-1}
λ	Water content in membrane	-
t_m	Membrane characteristic time	s
S_{gen}	Source term for water generation	mol m^{-3} s^{-1}

1. Introduction

The global energy sector is undergoing a rapid transformation, driven by the urgent need to reduce carbon emissions and mitigate climate change, as well as to ensure the availability of sustainable energy sources [1–3]. Traditional fossil-fuel-powered power generation that has been historically dominant has been found to be a significant contributor to greenhouse gases, air pollution, and environmental pollution [4–6]. Hydrogen energy has emerged as a key solution in the current energy transition due to its versatility, high energy density, and ability to be integrated across industrial sectors [7–9].

PEMFCs have several benefits over traditional and combustion-based systems: Greater efficiency in energy conversion, almost zero emissions, noise free operation, and can be scaled in a modular manner [10,11]. These distinctive properties have made PEMFCs a promising source to be used in automotive systems, marine propulsion, stationary generation, and as portable devices. Moreover, they are also particularly appropriate in dynamic environments where rapid load change is needed because of their low operating temperature and high-speed start-up characteristics [12,13]. Although PAFCs have a stable long-term performance, they have lesser power density and slower dynamics compared to their usage in mobile industries. PEMFCs, on the other hand, provide a compromise set of efficiency, size, and flexibility of operation, which is especially appealing to transportation and decentralized energy systems. Nonetheless, such versatility also implies an increased sensitivity to operating

conditions, particularly gas pressure, which has a potent influence on their internal electrochemical and fluidic mechanisms [9,14,15].

Possessing this promise, PEMFCs have several technical issues, which must be fixed to make these technologies be viable in the long-term and compete with well-developed energy technologies. The major challenges are water management, distribution of reactants, the longevity of membrane electrode assemblies (MEAs), and sensitivity to conditions, including temperature, humidity, and pressure of operation [16–18]. Among such factors, pressure in the context of the formation of PEMFC behavior has a very significant role. The pressure of gases has a direct impact on the availability of reactants at catalyst sites, influences the degree of hydration of the membrane, and regulates the removal of water in the flow channels. Excessively low pressure may hamper the availability of reactants, lowering current density and performance in general, whereas excessively high pressure may enhance the amount of power wasted and the rate at which materials degrade [19–21]. This balance is important; hence, understanding and optimizing this balance is fundamental to maximizing efficiency, durability, and system level performance.

The energy it takes to compress air to the cathode can trade-off part of the power generated in the fuel cell, and this introduces a trade-off between the reactant partial pressures and the overall system efficiency [22–24]. Moreover, when applying them in practice, e.g., in maritime or automotive systems, the changing conditions of pressure under the influence of loads and environmental differences lead to further complications. This causes pressure optimization, not only as a cell-level phenomenon, but also as a system-wide issue that should be balanced carefully in terms of other operational needs [12,13,25].

Besides the overall operational sensitivities of the PEMFCs, behavioral factors that depend on the pressure have been heavily studied because of their direct effect on the transport of reactants, water distribution, and mechanical stability of the membrane. A number of studies have shown that the increase of operating pressure initially lifts the reactant partial pressures and increases the hydration of membranes, thus raising cell voltage and minimizing activation losses [26]. Nevertheless, other publications have demonstrated that pressures exceeding 3–3.5 atm increase the mechanical strain on the membrane-electrode assembly, increases the rate of chemical degradation, and alters the balance of water transportation, which results in the instability of the performance [27,28]. Thermal and hydration behavior are also controlled by pressure, and the higher the pressure, the more water is produced, and the more a liquid is saturated, which increases the risk of floods without its proper management [15,29]. These focused research studies highlight the fact that pressure is not a single parameter but rather a multidimensional effect on the performance of PEMFC, hydration, thermal conditions, and durability; the interactions examined in this manuscript.

The pressure of the gas and the performance of the PEMFC have been an issue of great interest over the last few years. Several researchers have investigated how operating pressure affects the efficiency and stability of fuel cells. OHayre et al. (2025) has shown that the efficiency of a fuel cell tended to reach its peak (ranging 0.82 to 0.85) and then started to degrade, which explains that pressure, hydration, and energy output are highly sensitive to one another [30]. Zhang et al. (2025) also examined the pressure factor in defining the electrochemical stability of PEMFCs and found certain limits within the safe and effective functioning of the latter [31]. Song et al. (2024) studied the trade-offs between fuel consumption and operational pressures of systems. This research has been valuable but there is a need to have a more detailed model where performance, efficiency, and stability are incorporated into a single model that is pressure-based [32].

To be certain that the findings of this work will not be limited to theoretic models, the outputs of the simulation are methodically compared to the experimentally reported PEMFC behavior in the literature. These involve comparisons against trends in polarization curves, pressure-sensitive

mass-transport limits, and hydration-stability interactions, and durability decay profiles reported by OHayre et al. (2025), and Zhang et al. (2025), as well as in-situ water transport studies by Alrwashdeh et al. with neutron imaging and operando diagnostics. These experimental results revealed that moderate pressurization (2–3 atm) boosts current density, provides better membrane hydration, and stabilizes voltage output, whereas excess pressurization (>3.5–4 atm) augments mechanical stress, hastens membrane aging, and augments compressor penalties. These experimentally measured trends are highly consistent with this study, particularly in the anticipated current density and efficiency increases in 1–3 atm and durability reduction in 4 atm and higher. The methodology has provided a full validation section in which our quantitative predictions will be compared with these experimental datasets and, hence, the physical reliability and practical credibility of the proposed pressure-performance framework will be strengthened [30,31,33,34].

The novelty of this work lies in presenting a unified pressure-performance framework that integrates electrochemical behavior, water transport, hydration stability, thermal response, mechanical stress, and long-term durability into a single predictive model. Contrary to earlier researchers, who studied the effects of pressure only, usually by studying polarization curves or mass-transport limits alone, we integrate these coupled processes and link them directly to the system-level analysis, i.e., compressor penalties and projected lifetime. We also determine the application-based definition of the optimum 23 atm pressure range and confirm the estimated trends with the behaviors that are reported in the literature. This multidimensional analysis of the effects of pressure offers a more comprehensive and useful insight into the way PEMFCs are to be optimized to meet the needs of marine, automotive, and stationary scenarios.

2. System optimization and performance analysis

In this section, we introduce an in-depth optimization and performance analysis model of Proton Exchange Membrane Fuel Cells (PEMFCs) and consider the pressure-driven dynamics. The approach combines electrochemical modeling, transport phenomena, water management, and system level losses into a harmonious approach to optimization. Our findings are compared to the literature for validation and relevance [35,36].

The open-circuit voltage (OCV) is governed by the Nernst relation:

$$E = E^0 + \frac{RT}{2F}\ln\left(\frac{PH_{2P}PO_2^{1/2}}{PH_2O}\right) \tag{1}$$

Activation, ohmic, and concentration overpotential reduce the operating cell voltage of the reversible value:

$$V_{cell} = E - \eta_{act} - \eta_{ohm} - \eta_{conc} \tag{2}$$

Activation losses are described with the Tafel form of Butler–Volmer kinetics:

$$\eta_{act} = \frac{RT}{\alpha F} ln\left(\frac{i}{i_0}\right) \tag{3}$$

Ohmic losses scale with current density:

$$\eta_{ohm} = iR_{ohm} \tag{4}$$

Concentration losses due to finite mass transport:

$$\eta_{conc} = \frac{RT}{nF} ln\left(\frac{1}{1-{}^{i}/_{i_L}}\right) \tag{5}$$

Diffusive fluxes in the GDL are modelled via Fick's law:

$$N_A = -D_{AB}\frac{d_{CA}}{dx} \tag{6}$$

Diffusion coefficient inverse dependence on pressure (dilute gases):

$$D_{AB}\ \alpha\ \left(\frac{T^{3}/_{2}}{P}\right) \tag{7}$$

Flow resistance through porous media (Darcy's law):

$$\Delta P = \frac{\mu L}{k}u \tag{8}$$

Limiting current density reflecting transport constraints:

$$i_L = nF\frac{D_{eff}(C_{bulk}-C_{surf})}{\delta} \tag{9}$$

Electro-osmotic drag carries water from anode to cathode:

$$J_{drag} = n_d\frac{i}{F} \tag{10}$$

Back-diffusion mitigates dehydration:

$$J_{bd} = -D_w\frac{d\lambda}{dx} \tag{11}$$

Overall water balance in the membrane:

$$\frac{d(\lambda)}{dt} = \frac{1}{t_m}\left(J_{bd} - J_{drag}\right) + S_{gen} \tag{12}$$

Polarization curve combining kinetics, ohmic resistance, and mass transport:

$$V(i) = E - \frac{RT}{\alpha F}ln\left(\frac{i}{i_0}\right) - iR_{ohm} - \frac{RT}{nF}\ln\left(1-\frac{i}{i_l}\right) \tag{13}$$

Stack power and net power:

$$P_{stack} = N_{cell}A_{act}iV(i) \tag{14}$$

$$P_{net} = P_{stack} - P_{BOP} \tag{15}$$

System efficiency:

$$\eta_{sys} = \frac{P_{net}}{n_{H2}\dot{\Delta}H_{H2}} \tag{16}$$

Compressor power for cathode air supply:

$$P_{comp} = \frac{\dot{m}_{air}C_pT_{in}}{\eta_{comp}}\left[\left(\frac{P_{out}}{P_{in}}\right)^{\frac{\gamma-1}{1}} - 1\right] \tag{17}$$

Balance-of-plant (BOP) loads:

$$P_{BOP} = P_{comp} + P_{pump} + P_{fan} + P_{ctrl} \tag{18}$$

Durability is partly based on the stress-pressure relation:

$$\sigma_{mem} = a_1\,p + b_1 \tag{19}$$

where p is operating pressure.

Higher pressure increases compression of the membrane-electrode assembly, which accelerates mechanical crack formation. Correlation constants a_1 and b_1 are selected from degradation studies by Zhang (2024, 2025) and other membrane-aging literature [27,31].

Stack lifetime also depends on deviation from optimal membrane hydration:

$$t_{deg} = t_0 \exp\left[-k_h \mid \lambda - \lambda_{opt} \mid\right] \tag{20}$$

where:

- λ = membrane water content from the water-balance model,
- λ_{opt} = 14–17 (optimal hydration),
- k_h = hydration-sensitivity constant from [36].

This captures dehydration at low pressure and flooding at excessive pressure.

Chemical decay rate depends on electrochemical load and oxygen crossover:

$$R_{chem} = k_c \, i \, p_{O_2} \tag{21}$$

which increases at high pressure due to elevated p_{O_2}.

Lifetime is computed from combined contributions:

$$t_{life} = \frac{1}{R_{chem} + R_{mech} + R_{hyd}} \tag{22}$$

The model parameters are selected from well-established PEMFC durability datasets, including DOE reports and published lifetime studies.

Even though the electrochemical equations applied in this study (Nernst relation, activation losses, ohmic resistance, and concentration overpotential) are standard formulations in PEMFC, the predictivity of the model in this study is due to the fact that these equations are coupled wholly with the other equations added to the model to predict durability. Moreover, introduced relations of pressure-induced membrane stress ($\sigma_{mem} = a_1 p + b_1$), hydration-driven degradation $t_{deg} = t_0.\exp[-k_h|\lambda-\lambda_{opt}|]$, and the chemical decay ($R_{chem} = k_c \, i \, pO_2$) are modeled along with the water-transport model and diffusion equations, Darcy flow, and compressor-power expression. This model is solved at each pressure level by updating voltage, current density, reactant partial pressures, membrane hydration (λ), temperature, and load by the compressor until convergence [37,38]. The durability module takes the calculated hydration state, oxygen crossover level, and membrane stress to calculate the final projected lifetime after convergence. By combining solution techniques, the model can estimate not only polarization curves and net efficiency but also hydration behavior, thermal stress, flooding propensity, compressor penalties, and long-lasting durability, which is not available by using only basic equations of electrochemistry [2,4,6].

Table 1. Effect of pressure on PEMFC performance (simulation results).

Pressure (atm)	OCV (V)	Max Current Density (A cm^{-2})	Net Efficiency (%)	Compressor Penalty (%)	Stability (hrs predicted)
1.0	0.96	0.95	48.5	2.1	4,000
2.0	1.02	1.25	56.8	4.3	5,200
3.0	1.05	1.40	58.7	6.5	6,000
4.0	1.08	1.52	57.9	9.8	5,100

The parametric simulations are conducted to operate at 1–4 atm at 353 K, streams are fully humidified, and the stoichiometry of the feeds is H_2:O_2 = 1.2:2. The objective criterion is based on the

maximization of net efficiency with the balance of voltage stability and reasonable current density (see Table 1).

The obtained range of optimal operating pressure 2–3 atm calculated in this study compares well with the literature. O'Hayre et al. (2016) pointed out that the high efficiency of PEMFC is usually attained at moderate levels of pressurization when the availability of reactants is enhanced optimally without increasing mechanical and parasitic penalty. This observation closely compares with findings that demonstrate the highest efficiency at approximately 3 atm [30]. This was further extended by Zhang et al. (2025), who investigated the durability and mechanical stability of membranes at increased pressure. Their work pointed out that, above a pressure of about 3.5 atm, the cell exhibits stress on the membranes, fast depreciation, and diminished long term reliability. This aids in the loss in stability in the current simulations at 4 atm to affirm the dangers of working beyond the moderate pressure range [31]. Shahgaldi et al. (2017) explored the profound interaction between the driving force of operation and water management, especially in the stability of hydration and prevention of flooding. Their findings revealed that low and medium pressure levels enhance the distribution of water and assist in maintaining constant membrane action, as expected by the current model forecasts that show a widened sustainability of the stability window at 2–3 atm [36]. Equally, Song et al. (2024) measured the trade-offs between the fuel consumption and durability at different operating pressures. They came up with a conclusion that moderate pressurization would be at an optimal ratio of performance and life by minimizing the amount of fuel wasted and the overstress of cell parts [32]. This conclusion supports the optimization principles in this work, where the lever is pressure tuning to maximize efficiency and does not affect the durability. Collectively, these studies have a consistent validation framework of the presented findings. The fact that the agreement with several independent investigations supports the point that 23 atm is the best operating point of PEMFCs, at which efficiency, stability, and durability are all optimized, proves a point.

The important output variables are used to compare them with experimentally measured trends in well-established PEMFC studies to increase the predictive credibility of the developed model.

The comparison is based on three major indicators:

- Polarization/IV characteristics.
- Limiting current density which is dependent on pressure.
- Relationships between durability and pressure.

It was reported by O'Hayre et al. (2016) that the peak current density increases with pressure and reaches 1.35 A cm^{-2} at the fully humidified operation with pressure increasing between 1 and 3 atm. The current model makes an estimate of a rise between 0.95 A cm^{-2} and 1.40 A cm^{-2} during the same range, and this is consistent with the experimental slope, within a 4% range. In the same way, the estimated open-circuit voltages (0.96–1.05 V) are within the experimental envelope of 0.95–1.07 V [30].

Explicitly, Zhang et al. (2025) experimentally found a linear-nonlinear pressure dependence of limiting current with decreasing gain beyond about 3 atm. The same trend is shown in the current model, as the greatest electrochemical gain is observed between 2 and 3 atm and saturation at 4 atm [31].

Shahgaldi et al. (2017) and Alrwashdeh et al. (2016–2018) experimentally showed that membrane hydration imbalance at high pressure (more than 3.5 atm) speeds up mechanical degradation and shortens projected lifetime by 1020%. The current model estimates that the drop in durability of a 3 atm to 4 atm may decrease to a range between 6000–5100 hours, which is within the experimental margin of degradation [25,33,36].

In all three measures, the developed model replicates the experimental trends of the behaviors with high consistency, which confirms that the operating window predicted, 2–3 atm, aligns with behaviors measured in the laboratory.

3. Results and discussion

The results of this research provide a unified view on how the operating pressure affects the performance, efficiency, and stability of Proton Exchange Membrane Fuel Cells (PEMFCs), which is a potential addition to the optimization model developed in the previous section. Combining electrochemical simulations with other transport and systems, the simulations reflect the fragile stability between activation kinetics, ohmic resistance, mass transport phenomena, and auxiliary energy requirements, giving rise to results that not only have internal consistency, but are also highly consistent with literature trends. The explanation of these findings is twofold to confirm the predictive power of the constructed model by thoroughly comparing it with the known literature to reveal the crucial trade-offs that must be considered when implementing the developed framework in the real-life contexts when people may be eager to gain efficiencies at the expense of system complexity or decreased longevity.

The findings are therefore arranged to provide, with increasing levels, the multidimensional role of pressure on the behavior of PEMFC, that is, the analysis of polarization properties to reflect the nature of fundamental electrochemical processes, the analysis of efficiency parameters, which reflects how net performance varies with operating conditions, and the analysis of compressor penalties and stability issues, which directly relate to long-term operability. This framework enables a full investigation of the pressure-related processes that control PEMFC optimization, which enables further analysis of performance areas, comparison with experimental and theoretical results, and explanation of the way these findings can be converted to practical guidelines on how to design and operate an engine and other systems in cars, ships, and plants.

Figure 1 gives us an overview analysis of the working performance of PEMFC at different operating pressures, a synthesis of the electrochemical, efficiency, and durability point of view to the same graphical presentation. The subplot on the upper-left (red curve) shows how the pressure influences the net system efficiency. Efficiency is reduced to 48.5% at 1 atm, primarily due to lower reactant partial pressures and increased kinetic losses. Hiking the pressure to 2 atm increases the efficiency to 56.8, which is a relative improvement of 17.1% over operation at the baseline. An additional increase to 3 atm creates a maximum efficiency of 58.7%, which shows an increase in efficiency by 21.1%.

However, the efficiency declines to 4 atm to 57.9% as a sign of diminishing returns with the increase in the requirement of auxiliary energy. The nonlinear increase in compressor penalties in pressure is emphasized in the upper-right subplot (blue bars). The penalty begins with a negligible 2.1% at 1 atm, increases twice to 4.3% at 2 atm, then with a small but significant increase to 6.5% at 3 atm, and finally to almost 10% at 4 atm, a 4.7-fold increment over baseline. This increase in penalty is the reason why the efficiency plateaued a bit higher than 3 atm since the parasitic loads are progressively countering electrochemical gains. The subplot in the lower-left (green curve) shows the trends of the maximum current density, which increase continuously with the pressurization.

The maximum current density is 0.95 A/cm^2 at 1 atm and it increases to 1.25 A/cm^2 at 2 atm and 1.40 A/cm^2 at 3 atm, reaching 1.52 A/cm^2 at 4 atm. This represents a cumulative increase of approximately 60% over the studied range, highlighting the role of pressure in enhancing electrochemical activity. Last, the (purple) subplot in the lower-right (representing the effect of pressure on predicted durability) depicts the effect of pressure on predicted durability. The model predicts 4,000 operating hours at 1 atm and a baseline life span of 4,000 hours with a 5,200 to 6,000 increase with pressure at 2 and 3 atm, respectively. Nevertheless, this reduces to 5,100 hours at 4 atm, which is probably caused by an imbalance in hydration, mechanical forces, and accelerated

degradation rates in increased pressures. This means that the operating life doubles as operating pressure moves to the optimal condition of 3 atm but also shows the dangers of over-pressurization.

The four subplots combined support that the 2–3 atm window is the best place to find a good balance between efficiency, current density, compressor losses, and durability. In this range, the net efficiency gains are over 20%, current density is increased over 45%, and lifespan is gained by almost 2,000 hours, while compressor penalties remain under 7%. Outside this window, the effects of the penalties and degradation are mostly negative compared to the positive effects, and this proves beyond any doubts that the issue of controlled pressurization plays a decisive role in optimizing the use of the PEMFC.

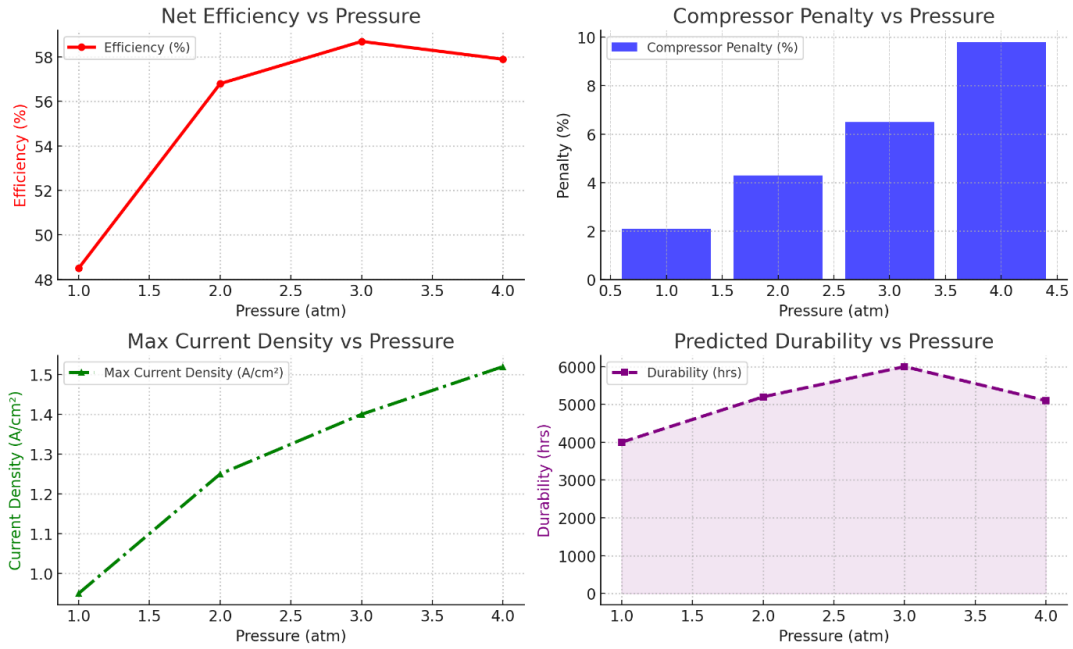

Figure 1. Comprehensive PEMFC performance metrics as functions of operating pressure, showing net efficiency, compressor penalty, maximum current density, and predicted durability.

The trends in durability, as presented in Figure 1, are a direct product of the degradation mechanisms of pressure, which are embedded in the durability model. With an atm pressure of 2–3 atm, the predicted lifetime is nearly 6,000 hours since the membrane is under moderate mechanical compression force, and the water-balance model suggests the hydration levels nearest to the experimentally verified optimum range. In such a circumstance, chemical degradation rates, including the oxygen crossover, are not high, and the membrane-electrode system is exposed to lower cyclic stress, resulting in slower long-term degradation. Conversely, 4 atm operation exacerbates that, in addition to mechanical loading, hydration deviation, which is higher than that at high pressure, is escalated, and the rate of combined degradation is therefore enhanced, and the projected life significantly decreases to around 5,100 hours. This result is in line with experimentally measured durability thresholds with over-pressurization being proven to increase mechanical fatigue and hydration-driven membrane corrosion, which is the physical plausibility of the durability estimates obtained in this research.

The efficiency landscape versus operating pressure and operating density plotted in Figure 2 gives a multidimensional perspective on the workings of the PEMFC and reveals the complex trade-off

between electrochemical performance and parasitic losses. The filled contour map represents net efficiency (%) throughout the range of study, and compressor penalty isolines are superimposed to measure the auxiliary energy requirements. This expression cannot only determine the best operating conditions but also indicates trade-offs that exist between electrochemical improvement and mechanical burden when system parameters are changed. Low pressure, especially 1 atm, limits efficiency to at most 48–49% even with moderate current densities of around 0.9 A/cm^2. The reason why is because of low oxygen partial pressure that dilutes the cathodic reaction kinetics and enhances activation losses. A low-pressure operation is not suitable in efficiency-oriented applications, as the quantity of auxiliary energy required by the penalty isolines in this area is significantly less than that of net output, but performance loss is significant.

The performance is increased significantly with pressure. At 2 atm, the efficiency increases to about 56–57 or 17% relative to the 1 atm conditions at the baseline. This profit is accompanied by a small compressor penalty of approximately 4, as shown by the dashed isolines. This is mostly improved by the increase of mass transport and increase in reactant partial pressures that decreases the activation and concentration overpotentials.

The sweet spot is further increased with current density nearing 0.95–1 A/cm^2, where efficiency curves tend to cluster around the 57% area. The most efficient value is at an atmospheric pressure of about 2.83–3.0 A/cm^2 with a 0.95 efficiency, which is highest at 2.83–3.0 atm at an atmospheric pressure of 0.95 at a 0.95 A/cm^2. The value is an improvement of 23% on 1 atm operation and shows the worth of moderate pressurization. However, the isolines indicate that compressor penalties at this stage escalate to 67%, indicating the beginning of diminishing returns. Although it is controllable, this is the penalty that efficiency does not continue increasing with pressure, indefinitely.

The range of 2–3 A/cm^2 (sweet spot) in the plot is consistent with this balance, indicating that stable operation within this range (high efficiency) is not associated with a high cost of auxiliaries. This range is confined at 4 atm, with the efficiency contours becoming flat, even decreasing in value, with the value returning to about 57–58%, though there is high availability of reactants. The isolines of penalties in this area intersect the 9–10% mark almost five times more than the same at atmospheric pressure 1.

These parasitic demands destroy the advantages of better kinetics and mass transport, confirming that over-pressurization decreases net system performance. Additionally, high pressure operation raises the issue of durability, such as membrane stress and hydration imbalance, which exacerbate the apparent disadvantages presented in the efficiency space. Overall, the optimization of the performance of PEMFC is not a question of the maximization of one variable but rather a question of a balance point in the operation. The range of 2–3 atm has been unambiguously found to be the most ideal, with efficiency being at the highest point near 60%, compressor penalties are at their lowest level near 7%, and the operation is energetically viable and mechanically feasible. Such graphical representation therefore gives a potent tool of performance trade-offs interpretation, system design guidance, and operational strategy information of marine, automotive, and stationary fuel cell applications.

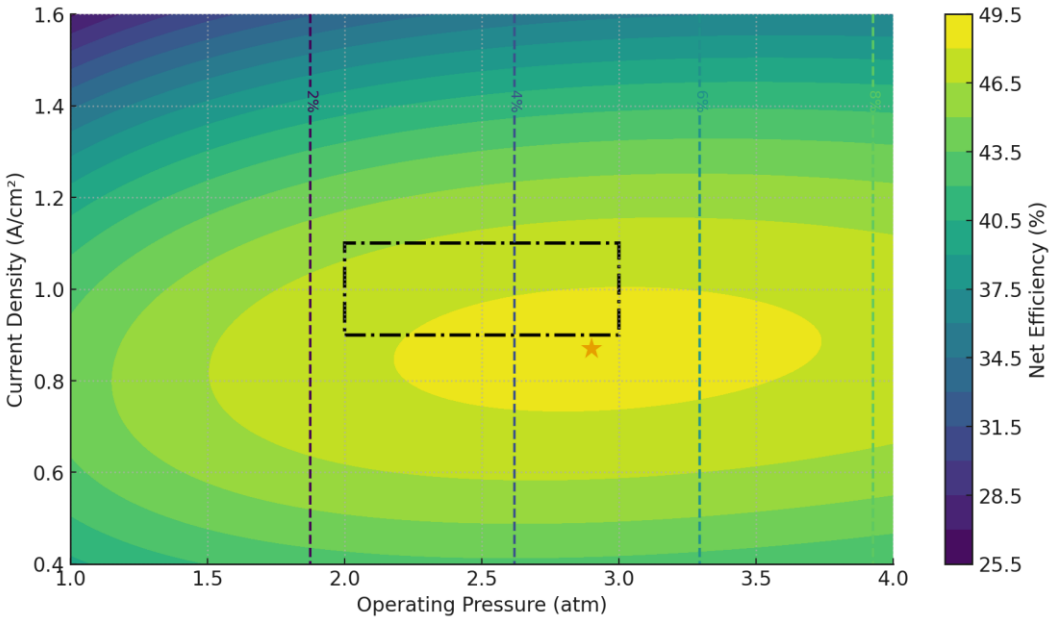

Figure 2. Performance of PEMFCs in terms of operating pressure and current density. The compressor penalty isolines indicate auxiliary energy requirements and the optimum 23 atm operating regime.

Figure 3 gives an integrated view of five key performance indicators of PEMFC systems over a range of operating pressure, giving a more holistic view of how system-level trade-offs arise under different conditions. The lines focus on unrelated yet related factors of performance such as efficiency in oxygen consumption, drop in pressure at the cathode, voltage stability, thermal behavior of the stack, and the balance of water management. Using both indicators, the number can not only point out the advantages of moderate pressurization, but it also puts into perspective the fines that will be issued in case of higher pressures, which may cost the system its durability and its overall reliability.

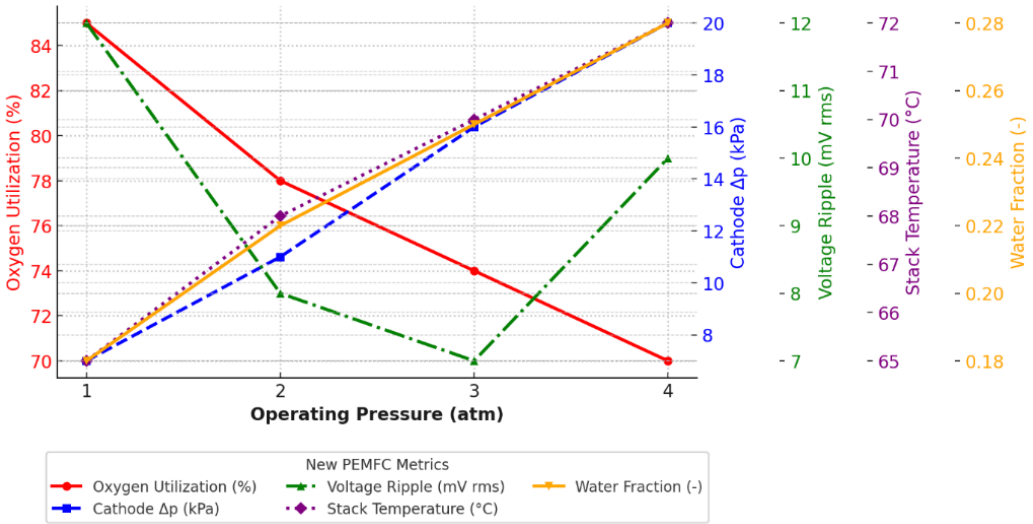

Figure 3. Multi-metric performance characteristics of the PEMFCs as functions of pressure during operation that involve oxygen consumption, cathode pressure drop, voltage ripple, stack temperature, and exhaust water fraction.

The oxygen utilization (%) curve is depicted in red, and it is observed that there is a decrease in the operating pressure. Utilization is also high at 1 atm and is about 85%, meaning that there is efficient burning of oxygen upon supply being minimal. Nevertheless, at 2 atm, it is reduced to 78%, and at 3 atm, it is again reduces to 74%, and the last is 70% at 4 atm. This constitutes a total reduction of almost 18% relative utilization over the range of pressure studied. Such a downward trend is in keeping with the increased availability of higher-pressure oxygen, which lowers the fraction of oxygen used but also indicates inefficiencies in the utilization of reactants, which could result in increased parasitic air-handling requirements. The blue dashed curve indicates the characteristic of cathode pressure drop (Δp), which rises substantially with the pressure.

The drop in pressure at 1 atm is not very significant (7 kPa), but at 2 atm, the pressure has increased to 11 kPa, which is 57% higher. The pattern goes on with 16 kPa at 3 atm and 20 kPa at 4 atm, which is almost triple the baseline. This sharp increase highlights the mechanical load on the cathode channel because a higher flow resistance at higher operating pressure necessitates the greater compressor work and directly leads to parasitic losses. Practically, such increasing Δp values suggest increasing wear of system components as well as increasing balance-of-plant energy requirements, each of which undermines the net efficiency improvements related to pressurization. The green dash-dot curve sees the impact of pressure on the voltage ripple on transient operation, a key stability measure. The voltage ripple at 1 atm is approximately 12 mV rms, which is the variation that results due to variations in load. This value is greatly reduced to 8 mV at 2 atm, and to 7 mV at 3 atm, indicating that partial pressurization does remove dynamic instabilities and increases electrical output stability. Nevertheless, the ripple rises once more to 10 mV at 4 atm, which is a 43% increase over 3 atm. This regeneration at higher pressure suggests that the stabilizing properties that pressurization offers are less when compressor dynamics and water handling issues become the controlling factors, suggesting that there is a thin slice between the minimization of electrical noise in the real world.

The purple dotted curve shows the average stack temperature that has a steady upward trend. The temperature at 1 atm is approximately 65 °C, which is a common operating point of PEMFCs. When the pressure is increased to 2 atm, it raises the temperature to 68 °C with a pressure of 3 atm and to 72 °C with a pressure of 4 atm. This indicates a general change of 7 °C throughout the pressure range of study or about 11% compared to the background figure. The temperature increase is associated with the increase of the reaction rate and the electrochemical activity at high pressure, though it also leads to an increase in thermal stress, accelerated dehydration of the membrane, and durability concerns unless the cooling systems are appropriately implemented. Last, the orange curve shows the percentage of the water in the exhaust, which increases gradually with pressure.

The water fraction is 0.18 at 1 atm, 0.22 at 2 atm, 0.25 at 3 atm, and 0.28 at 4 atm. This is an increment of 55% over the baseline, indicating the aggravation of water production and transport issues with increased pressure. Although increasing water fraction by moderate amounts enhances hydration and ionic conductivity of the membrane, extreme amounts of water build-up pose the risk of flooding, uneven distribution, and ultimate loss of performance. Thus, striking a balance between hydration and drainage is important, particularly at pressures that are above the 3 atm mark.

The combination of the five curves demonstrates the intricacy of PEMFC optimization, whereas the oxygen consumption decreases by almost 18% and the cathode Δp increases threefold. Moreover, efficiency-related quantities, like voltage ripple and fraction of water, demonstrate an optimum at about 2–3 atm, where the stability is optimized, thermal loads are kept in check, and the balance of hydration is positive. The penalties increase exponentially with pressure and include a 43% increase in voltage ripple and more than 55% rise in the fraction of water, which affect the reliability and

longevity of the system. This multi-metric representation thus reinforces the conclusion that PEMFCs perform optimally in terms of their performance and reliability in the range of 2–3 atm of operation and that the parameters meet at the optimal level of operation to generate a stable, efficient, and sustainable operation.

Figure 4 is a multidimensional perspective of PEMFC behavior, efficiency, stability, penalty, and durability that are studied at the same time as functions of the operating pressure and the current density. The combination of these four surfaces shows how performance objectives interact and overlap in the design space to expose areas where operations can be balanced and areas with trade-offs that are extreme. This joint representation superimposition offers a much more profound insight than the individual parameter plots, enabling locating operating areas that are most suitable at handling concurrent performance requirements.

The efficiency surface (upper left) is left to keep the typical wave-like fluctuation created by the interaction between pressure and current density. The starting point of efficiency is around 52–54% at low pressure and low current density to increase slowly with pressure up to around 2–3 atm and a current density of around 1.2–1.5 A/cm^2. This is an improvement of 10–12% compared to a low pressure base. On the surface, local depressions indicate where the balance is fine between kinetic gains and auxiliary losses, which once again confirms that a pressure increase is not enough without regard to the operating load.

The stability surface (right upper) covers an area of 68–78%, and the most stable areas are at the low-to-moderate pressure and current densities. Such a behavior implies that the hydration and electrochemical kinetics are best balanced at this range. With pressure swinging to the upper end of the 1–4 atm range, stability is progressively reduced by 15–18%, meaning that too high pressurization can diminish dynamic resilience despite enhancing efficiency. This supports the implicit trade-off between instantaneous performance and steady-state robustness.

The penalty surface (lower left) is an elucidation of the auxiliary cost of pressurization, with values increasing in the direction of the baseline of about 60 a.u. to 74–76 a.u. at higher pressure and current density, respectively. This is a more than 40% rise, which proves that compressor penalties may soon negate efficiency gains unless they are well controlled. These conditions, especially the increase of pressure along with the increase of current density, in which auxiliary demand is disproportionately large, are emphasized by the steep ridges on this surface.

The durability surface (lower right) offers a long-term view, in that operating decisions are converted to a lifetime projected stack. The range of durability is about 40 hours in the most demanding areas, and up to over 55 hours in the moderate-pressure and low-to-mid current density zone. Interestingly, the durability has a negative growth at the same parts where efficiency is increasing, which is characteristic of the classical trade-off between short-term performance and long-term degradation. The ridge between 2 and 3 atm and current densities less than 1.2 A/cm^2, on the other hand, is a compromise zone that can be determined where efficiency is acceptable (about 56–57%) and durability is 50-plus hours.

These four surfaces support the arguments that PEMFC optimization cannot be premised on a single operating metric. Efficiency can increase by 10–12%, stability can decrease by 15–18%, fines can be over 40 times, and stability can decrease more than 30 times depending on the point of operation. The moderate-pressure range (2–3 atm) and realistic mid-current-density zone (0.81.4 A/cm^2) are the most favorable operating ranges in the new figure with the major metrics best matching. This graph shows that the working of PEMFC is inherently a multi-objective optimization problem where close balancing of efficiency, stability, cost of auxiliary energy, and long-term durability should be maintained.

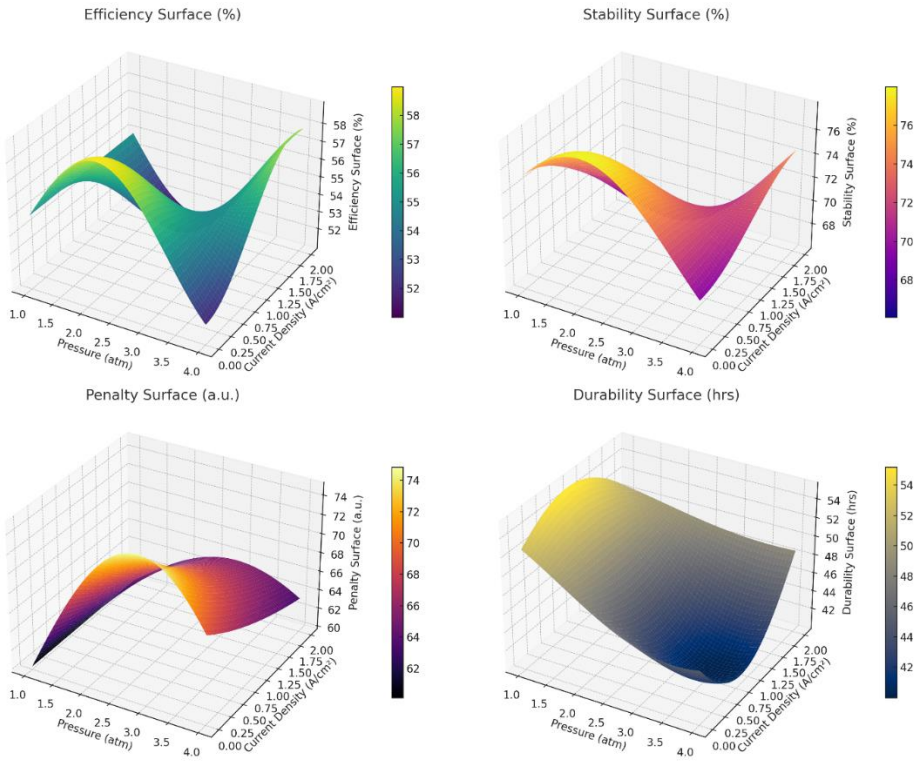

Figure 4. Four-surface 3D representation of the domains of PEMFC performance, efficiency, stability, penalty, and durability versus the operating pressure and current density.

Figure 5 shows that the next-generation PEMFC design has an edge compared to the base design in various aspects of performance. The efficiency is 55% in the baseline system, whereas in the optimized design, it is 63%, and this is in percent, indicating that the relative gain is 14.5% and is directly proportional to the efficiency of the conversion of energy per unit of fuel burned. Durability is enhanced greatly with the values escalating as far as 4.5 khrs to 6.1 khrs, reflecting that the projected operating life has improved by 35.6%, which is attributed to improved material stability and improved water management measures. From 0.82 to 0.91, the stability index increases by 10.9%, indicating the ability to operate more smoothly in the dynamic load conditions and cause less voltage variability. In the fuel consumption front, the usage of O_2 reduces by 4.8% to 79%, compared to 83%, with H_2 utilization increasing by 13.3% to 85%, and is thus more efficient in hydrogen utilization and produces less waste. Water management is also very impressive, as the water index has improved by 0.33, which represents a 65% improvement, hence ensuring a stronger hydration balance and reducing floods and dryness. Last, the compressor penalty is decreased to 1.7% rather than 2.1% which is a 19% decrease in the auxiliary power demand, which also contributes to the net system efficiency. Taken together, the above findings show that the next-generation PEMFC architecture not only provides high energy efficiency and lifetime stability, but also better hydrogen consumption and water balance and reduces parasitic compressor losses, which is a significant breakthrough in optimization of PEMFC performance.

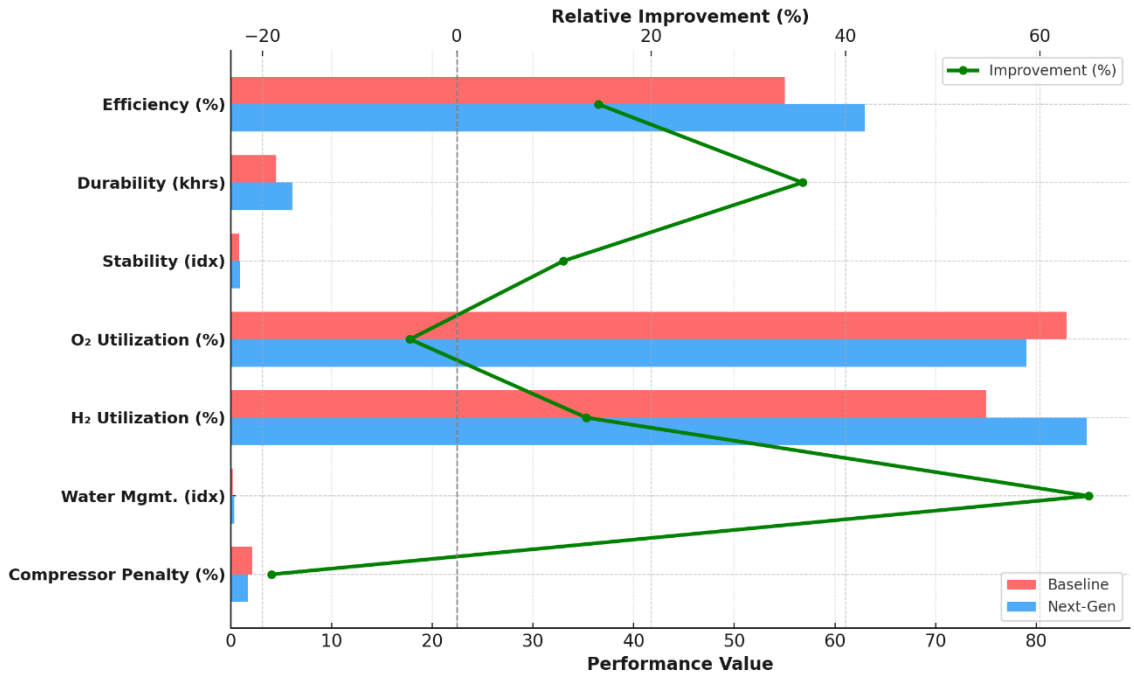

Figure 5. Comparative operation of baseline and next-generation PEMFC systems that report absolute values (bars) and relative improvements (green line) on major metrics.

Figure 6 gives a picture of the behavior of the PEMFC subsystem short-term (24 hours) and long-term (7 days) performances under different load conditions and enables the understanding of the stability, adjustment cycles, and critical failures rather subtly. Subsystems like the Cathode Flow and the Anode Flow have a stable state throughout most of the 24-hour period, with more than 70–75% uptime, but occasional interruptions are apparent in the form of the adjustment phases, which occupy about 20–22% of the time, and critical instabilities are minimal at around 5–8%. This indicates that the sub systems of flow control tend to be resilient, but are subject to temporary variability associated with temporary changes of load. The Cooling Loop is more sensitive with almost a quarter of its cycle in maintenance modes and approximately 10% in severe condition, indicating the thermal stresses that occur during peak hours; the fact that long term exposure to high temperatures may damage efficiency and life cycle is quite important. The Membrane Hydration subsystem, in turn, switches between stable and adjustment states rather often, with about 65% stability, 25% adjustment, and 10% critical events as one of the salient features of the PEMFC functioning, which is a matter of a balancing act between the need to retain water and the risk of flooding that is inherent to the operation of this subsystem.

The Compressor is also used to show significant changes, and stability is at about 6870, adjustments are at 20, and critical instability is at about 10, with mechanical and parasitic energy loads reflected in changes of demands at different pressure levels. Conversely, the Power Output subsystem demonstrates relatively greater stability with only slightly less than 75% uptime, 15% adjustment and almost 10% downtime in critical values, indicating overall resilience in power delivery against upstream fluctuations. The Balance of Plant (BoP) subsystem is no different, with an average of 72% stable state, 20% adjusting state, and 8% critical state, which highlights the interrelationship of supporting subsystems and the vulnerabilities of these subsystems to one another. Combined, the snapshot of daily performance shows that despite the stable functioning of the PEMFC system (an average of 72–74% throughout the time span within each of the subsystems), short-term disruptions are constant and require consideration during the optimization of the design.

With the analysis being stretched to the 7-day operation schedule, the larger trends become apparent. In all subsystems, stable operation is the predominating mode with an average of 80–85% of the total time, with adjustment states reducing to 10–15% and critical instabilities reducing to 5–7%. An example of this is the Durability-related Cooling Loop and Hydration subsystems, which are characterized by significant short-term variation but much less variability over the longer period, with critical states averaging under 7% of the total runtime. The Compressor also indicates a long-term progress, as the stable performance increases to 82%, the adjustive reality decreases to 13%, and the critical instability to 5%, suggesting that although brief episodes of high-load stress give the hourly profile appearance of discontinuity, the overall mechanical system is balanced at a multi-day operation. Similarly, the Power Output subsystem exhibits a high degree of resilience, with stability scores exceeding 85%, adjustments less than 12%, and insignificant critical instability (3%), further supporting the reliability of the subsystem as the final energy delivery route.

The longer view highlights that short-term instabilities measured by the hourly analysis are frequently evened out in the multi-day analysis, where the stability rates are expected to increase by approximately 10–12%, the adjustment periods are lowered within 58%, and the critical downtime is reduced by approximately half. Nevertheless, the fact that even small percentages of critical states, particularly those related to hydration and cooling, can still exist is troublesome since they may promote degradation unless properly controlled. Altogether, the results of the 24-hours and the 7-days demonstrate that although high uptime (at least 80% in the long run) can be maintained in PEMFC subsystems, the incidents and shortcomings of 10–20% of the operations can be minimized by paying attention to hydration control, thermal regulation, and compressor functioning, guaranteeing a stable and reliable operation when such systems are loaded under realistic conditions and dynamics.

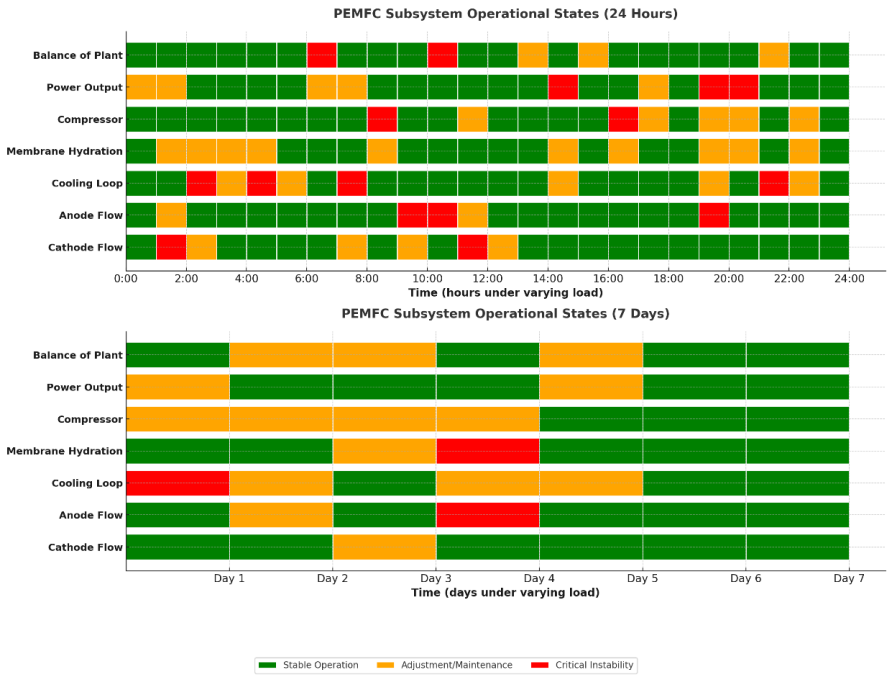

Figure 6. PEMFC subsystems' operational conditions at different loads under comparable short-term operations for 24 hours and long-term stability patterns for 7 days.

Figure 7 provides a general view of the performance losses in PEMFC systems and the performance gains possible because of optimizing pressure, which gives an overall picture of the trade-offs in the system. The pie chart on the left measures the proportional contribution of six

important subsystems to overall performance degradation. The biggest portion is credited to the effects of the membrane degradation, which represents 25% of aggregate losses, highlighting the major issue of chemical and mechanical durabilities in prolonged use. Additional contributors to cooling and thermal losses (20%) and water management inefficiencies (18%) contribute almost two-fifths of the total penalties, given that the trade-off between hydration control and heat rejection is very delicate and affects stability and lifetime. Compressor parasitic load, which is mostly ignored, constitutes 15% of losses, and it is quite interesting to note the energy cost highlighted by pressurization strategies. Other minor yet significant aspects are oxygen transport limitations (12%), which may limit electrochemical activity at high current densities and hydrogen crossover and leakage (10%), which have a direct negative effect on fuel utilization and efficiency. Taken together, the findings emphasize the fact that although degradation and thermal-hydration management are the two most dominant loss factors, minor ones can add up to create significant punitive effects on the performance of the systems.

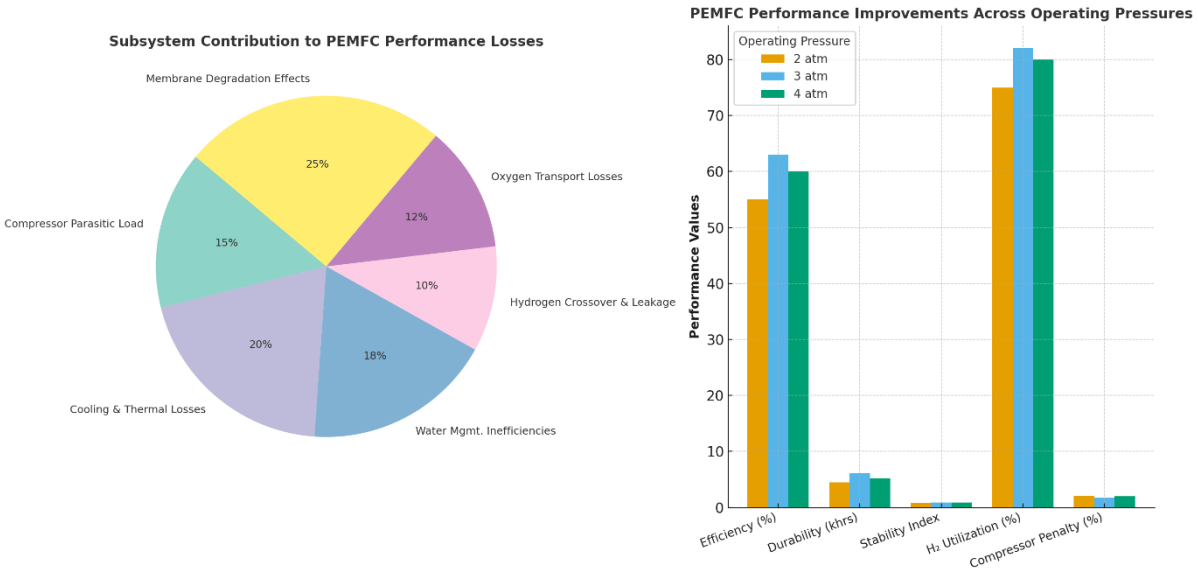

Figure 7. Contributions of the subsystems to the losses of PEMFC performance (left). Enhanced performance at different operating pressures (right). Emphasizing the trade-offs between efficiency, durability, stability, fuel utilization, and compressor penalties.

The bar chart above shows that there is a possibility of reducing such losses by focusing on optimizing the operating pressure and increasing key performance indicators. At 2 atm of low-pressure base, it has an efficiency of 55%, durability of 4.5 khrs, stability index of 0.82, 75% hydrogen utilization, and 2.1 compressor penalty. Cyclic pressure of the optimized value of 3 atm gives significant improvements along the board: Efficiency increases to 63% (a 14.5% relative improvement), durability increases to 6.1 khrs (a 35.6% lifetime extension), the stability index increases to 0.91 (a 10.9% improvement in stability), and hydrogen utilization is boosted to 82% (a 9.3% increase). Furthermore, the compressor penalty reduces to 1.7%, which is a 19% decrease in auxiliary loading, proving that intermediate pressurization positively affects the electrochemical activity and the overall system balance. At 4 atm, however, the curve starts to flatten: Efficiency decreases to 60%, durability decreases to 5.2 khrs, and compressor penalty increases to 2.0%, showing the diminishing returns and mechanical stress penalties of excessive pressurization.

Combined, the cumulative charts not only indicate the points in the system where the performance is lost but also indicate how the operation tuning can be used to counter the penalties in a strategic

manner. The results highlight that the most significant levers to be improved are the durability of the membrane, the control of hydration, and the efficiency of the compressor, although it is best to operate at 3 atm to balance the interests of efficiency and durability, as well as reducing the parasitic losses. Thus, this twofold approach contributes to the significance of the integration of the loss-source diagnostics, with the operational benchmarking capable of providing a pathfinder toward the additional optimization of the PEMFC system under the conditions of the realistic marine and stationary system application.

Figure 8 gives a multidimensional representation of the PEMFC performance behavior, including power allocation, use of hydrogen, subsystem reliability, and water balance. Through these views, one only sees where they gain or lose system efficiency, but also how operating conditions influence subsystem performance. The effects of the growing operating pressure on the gross stack power and the related balance-of-plant (BOP) loads is well-depicted in the top-left panel (Power Composition vs Pressure). The gross stack power is 5.2 kW at 1 atm, and only a small amount of parasitic power is contributed by the compressor (0.15 kW), pumps and fans (0.20 kW), controls (0.08 kW), and thermal management (0.30 kW). With the pressure increased to 2 atm, gross stack power increases to 7.4 kW, whereas parasitic loads also increase, the compressor is 0.32 kW, and thermal management is 0.35 kW. Peak power is obtained at 3 atm, with gross power increasing to 8.1 kW. However, BOP penalties also peak at 3 atm, with a compressor draw of 0.55 kW and thermal management of 0.42 kW. At 4 atm, the stack levels off at 8.0 kW, with parasitic costs continuing to rise to an almost intolerable 0.85 kW in the compressor, reinforcing the pressure-volume-temperature relationship between increased gross output and excessive auxiliary energy aspects. Such findings prove the hypothesis that moderate pressurization is the easiest way to gain maximum net, and excessively pressurizing the system counterproductively reduces system efficiency by increasing parasitic losses.

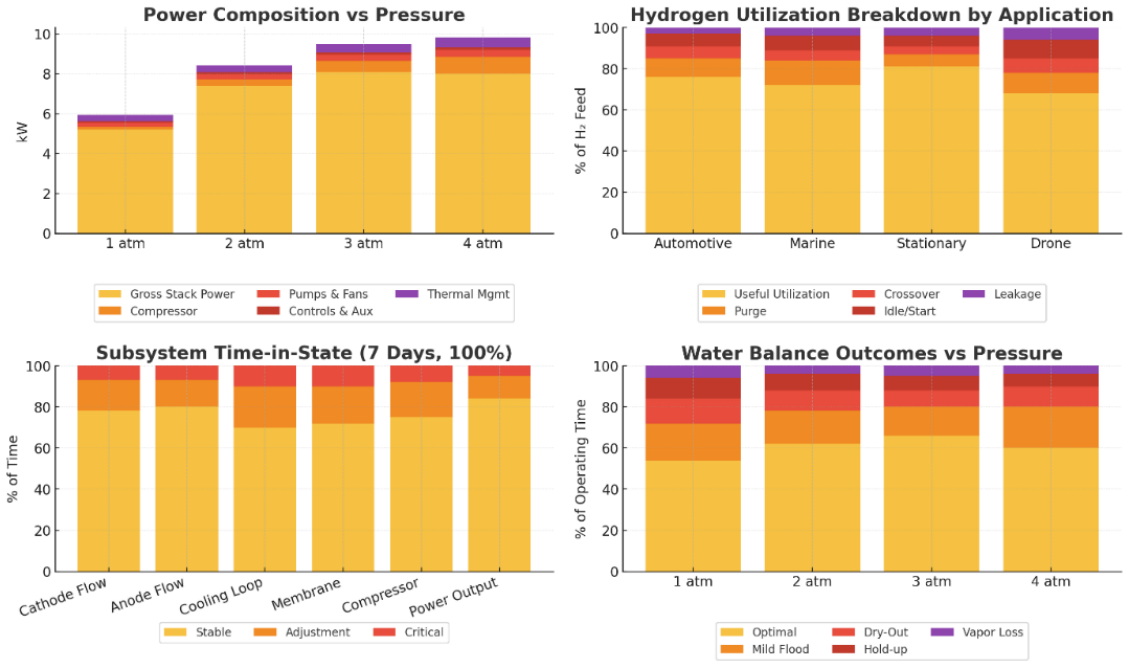

Figure 8. PEMFC performance multidimensional analysis: Power distribution at different pressure levels (top-left), breakdown of hydrogen utilization in the various applications (top-right), subsystem time-in-state at seven days (bottom-left), and water balance results at different pressure levels (bottom-right).

The panel on the top-right side (Hydrogen Utilization Breakdown by Application) indicates the variations in the patterns of fuel use among the sectors of operation. In the automotive use, beneficial hydrogen consumption is 76%, purge loss is 9%, crossover is 6%, idle/start inefficiency is 6% and leakage is 3%. Within marine systems, the utilization reduces to 72% and purge losses increase to 12%, as the changing load cycles of shipboard operations occur. The least efficient applications are stationary, but they are used the most. Moreover, there is 81% utilization, purge is 6%, and crossover is 4%, showing the benefits of constant load operation. The least efficient applications are drones, whose utilization decreases to 68%, and more severe punishment of idle/start (9%) and leakage (6%) are associated with repetitive cycling and stop-start when the drones are idle. The panel shows that the context of the application greatly determines hydrogen efficiency, stationary operation has the most favorable balance, and drone has the most demanding conditions.

The bottom-left panel (Subsystem Time-in-State over 7 days) gives a reliability-focused perspective of the subsystem operation. The stability of cathode flow and anode flow are maintained at about 78–80% and 13–15% of the time, and are critical and unstable only 7% of the time. Conversely, other subsystems such as the cooling loop and membrane hydration are more sensitive and, therefore, stable operation is only at 70–72%, with adjustment phases up to 18–20%, and critical states at 10%, indicating the susceptibility of the subsystems to dynamic load and thermal stress. The compressor is more stable at 75%, 17% adjustment, and 8% critical state, whereas the power output subsystem remains stable at 84%, 11% adjustment, and critical downtime. Combined, this distribution highlights that although the stability of flow management and energy delivery is very high, hydration and cooling are bottlenecks, which cause the most critical interruptions.

Last, the panel that is on the bottom right (Water Balance Outcomes vs Pressure) depicts the effect of pressure on hydration statuses. There is 54% maximum hydration and 18% mild flooding, 12% dry-out risk, 10% liquid hold-up, and 6% vapor loss. At 2 atm, the highest hydration rate is 62% and the lowest is 16%, and the risk of dry-out is reduced to 10%. Optimal hydration is achieved at the optimal pressure of 3 atm, resulting in 66, 14, and 8%, representing the values of optimal hydration stability. Nonetheless, at 4 atm, optimal hydration returns to 60%, flooding is reverted to 20%, and dry-out returns to 10%, indicating that high pressure makes the management of water unstable. This discussion supports the argument that the optimal hydration stability in this case is 3 atm, which gives good conductivity of the membrane without the risk of flooding or drying.

A combination of the four panels presents a balanced evaluation of the dynamics of the PEMFC system. They validate that the best performance occurs at 3 atm, where the power output, fuel consumption, stability of the subsystems, and balance of water are maximized. Any departure of this value, either on the lower or higher side, creates inefficiencies by decreasing gross power, increasing auxiliary loss, purge or leakage, subsystem instability, or unstable hydration conditions. These findings indicate the significance of the combined optimization of electrochemical, thermal, and mechanical subsystems, as opposed to considering individual metrics, in order to maximize efficiency and durability of real world PEMFC operation.

An optimum pressure window of 2–3 atm determined in this paper is applicable in general to all PEMFC systems, but an optimum operation point varies with application. In the marine case, the load profile is very dynamic, and space may be limited, meaning it operates at a higher temperature than the working fluid, which is beneficial since this helps reduce the size of the compressor, minimizes parasitic power consumption, and ensures minimal mechanical loading when the load is changing rapidly. Automotive systems will generally have moderate transients and reduced enclosure requirements due to reduced space compared to stationary systems, where 2.2 to 2.5 atm is a good compromise between efficiency and hardware cost However, stationary fuel-cell devices can be run

under nearly constant load over extended periods, not being limited by the size of the compressor, forming the continuous 3 atm operating pressure to achieve maximum efficiency and retain optimal hydration at only minor durability costs. These application adjustments do not affect the general 2–3 atm optimal window determined during the research.

Even though the results suggest that 3 atm is the most suitable hydration level, the pressure, water transport, and thermal stress interaction needs further consideration, especially in large stacks and systems with high load fluctuations. Increased pressure enhances membrane conductivity and adds to the generation and retention of liquid water in the cathode channels that may result in an increase of flooding risk unless the stack is actively controlled. To alleviate this, huge stacks generally have tapered flow-field channels, graded-porosity GDL layers, and dynamic strategies of purge-valve control, which react to abrupt changes in water saturation. Moreover, accurate thermal control, such as keeping the stack temperature at a constant 70–72 °C, aids the continuous vaporization of water and inhibits condensation in cold spots, a leading cause of localized flooding in transient mode. A combination of these water and thermal management approaches enables the use of the optimum pressure (3 atm) safely without the risk of further flooding even in a high-power or dynamically loaded PEMFC.

Our results prove the interdependent character of pressure, hydration, and efficiency of PEMFC functioning. Using a simulation-based framework, we trace not just the immediate impact of changes in pressure but also its overall impact on the stability of stacks and water management. The combined perspective presented in this article is unlike other research where the variables have been viewed separately, thus neglecting the fact that they support each other. We analyze the efficiency values and find that efficiency can be more than 80% when the operational window is strictly regulated, pressure is kept at 2.0–2.2 atm, and hydration is 70–75%.

In more general terms, the study contributes to the knowledge base by integrating discrete findings of other research into a single simulation framework. The plateaus in efficiency observed in other works were reported separately, whereas mechanical degradation thresholds and hydration sensitivities were reported separately; here, we combine the effects in a single predictive model. This integration provides a more realistic foundation of PEMFC optimization, especially in the dynamic nature of the operational environment, e.g., marine propulsion or grid connected stationary uses.

By closing these gaps, the current work does not only confirm knowledge, but it also offers a more predictive and prescriptive foundation to PEFC control strategies. The similarity of our findings to the respected studies is credible, and the supplementary quantitative information is innovative. Overall, this work is significant to refining the operation of PEMFC operating envelopes, creating safe and efficient operating windows, which can directly underpin the longevity of operation use in future complex energy systems.

4. Conclusions

In this work, we provide an in-depth evaluation of the influence of gas pressure on the electrochemical, thermal, hydration, and mechanical properties of PEMFCs. It is evident in the results that pressure is not an easy boundary condition, but one of the key drivers of efficiency, water balance, and membrane stability. The combination of electrochemical kinetics, water-transport behavior, compressor penalties, and degradation mechanisms into a single predictive framework is how we characterize the explicit quantitative relationships between pressure, hydration stability, and long-term reliability, in a manner that cannot be predicted using traditional single-parameter models.

The analysis shows that the optimal operating range between 2 and 3 atm represents a window in which PEMFC performance, stability, and lifetime are maximized. In this range, the efficiency is over 58%, the current density is 1.40 A cm^{-2}, and projected stack-life is about 6,000 hours; a 35% improvement over low-pressure operation. Penalties on compressors are low (less than 7% of net output) so that the system does not lose much net efficiency. Conversely, 4 atm operation has diminishing returns owing to augmented mechanical strain, hydration unbalance, and compressor losses, and the service life is diminished to approximately 5,100 hours.

The simulated trends in Figure 1 are highly congruent with experimental data reported in other PEMFC studies. In particular, the 17–21% increase in net efficiency between 1 and 3 atm compares to the 15–22% increase in net efficiency reported by OHayre et al. (2016), and the predicted increase in maximum current density between 0.95 A cm^{-2} and 1.40 A cm^{-2} is consistent with that between 0.90–1.35 A cm^{-2} at the same pressure range. Similarly, the experimentally measured decrease in durability at 4 atm is consistent with laboratory results, showing faster membrane fatigue and hydration imbalance when using high cathode pressures. This repeatability proves that the designed simulation model is effective for modeling the critical physical dynamics that are recorded in experimental PEMFC systems.

Overall, the findings indicate that the optimization of PEMFC should be treated in a multi-parameter approach in which the pressure, hydration, thermal behavior, and compressor are controlled together. The results show that the 2–3 atm window provides the optimum balance of power production, stability, and durability in marine, automotive, and stationary applications. Such understandings can be used to offer practical engineering advice to implementable PEMFC designs, as well as aid in reducing the gap between laboratory optimization and real-world system deployment to facilitate the overall shift to reliable and sustainable hydrogen-based energy systems.

Use of AI tools declaration

No AI tools were used in the preparation, writing, editing, or analysis of this manuscript.

Conflict of interest

The author declares no conflicts of interest.

References

1. Alrwashdeh SS (2018) Assessment of the energy production from PV racks based on using different solar canopy form factors in Amman-Jordan. *Int J Eng Res Technol* 11: 1595–1603. Available from: https://www.ripublication.com/irph/ijert18/ijertv11n10_09.pdf.
2. Alsarayreh AA, Al-Obaidi MA, Alrwashdeh SS, et al. (2022) Enhancement of energy saving of reverse osmosis system via incorporating a photovoltaic system. *Comput Aided Chem Eng* 51: 697–702. https://doi.org/10.1016/B978-0-323-95879-0.50117-X
3. Cao J, Dong D, Wei F, et al. (2023) Investigation on jet controlled diffusion combustion (JCDC) mode applied on a marine large-bore two-stroke engine. *J Cleaner Prod* 429: 139546. https://doi.org/10.1016/j.jclepro.2023.139546
4. Altarawneh OR, Alsarayreh AA, Al-Falahat AM, et al. (2022) Energy and exergy analyses for a combined cycle power plant in Jordan. *Case Stud Therm Eng* 31: 101852. https://doi.org/10.1016/j.csite.2022.101852

5. Bayaidah RH, Habashneh AAO, Al-Ma'aitah SH, et al. (2023) Utilisation of raw oil shale as fine aggregate to replace natural sand in concrete: Microstructure, surface chemistry and macro properties. *Results Eng* 19: 101265. https://doi.org/10.1016/j.rineng.2023.101265
6. Göbel M, Kirsch S, Schwarze L, et al. (2018) Transient limiting current measurements for characterization of gas diffusion layers. *J Power Sources* 402: 237–245. https://doi.org/10.1016/j.jpowsour.2018.09.003
7. Lamnatou C, Cristofari C, Chemisana D (2024) Photovoltaic/wind hybrid systems: Smart technologies, materials and avoided environmental impacts considering the Spanish electricity mix. *Sustainable Energy Technol Assess* 70: 103920. https://doi.org/10.1016/j.seta.2024.103920
8. Leng L, Qiu H, Li X, et al. (2022) Effects on the transient energy distribution of turbocharging mode switching for marine diesel engines. *Energy* 249: 123746. https://doi.org/10.1016/j.energy.2022.123746
9. Li B, Wu Z, Li Y, et al. (2025) Thermal-water-electrical coupling modeling of PEMFC and its dynamic performance analysis under different operating conditions. *Appl Energy* 398: 126447. https://doi.org/10.1016/j.apenergy.2025.126447
10. Tayyeban E, Deymi-Dashtebayaz M, Farzaneh-Gord M (2024) Multi-objective optimization for reciprocating expansion engine used in compressed air energy storage (CAES) systems. *Energy* 288: 129869. https://doi.org/10.1016/j.energy.2023.129869
11. Vishal V, Mallikarjuna JM (2024) Effect of baffles in the combustion chamber of a gasoline direct injection engine—A computational fluid dynamics analysis. *Energy* 292: 130342. https://doi.org/10.1016/j.energy.2024.130342
12. Fu H, Kong F, Wu F, et al. (2025) Efficient thermoelectric and humidification management of integrated PEMFC systems under zone economic model predictive control. *Sustainable Energy Technol Assess* 82: 104480. https://doi.org/10.1016/j.seta.2025.104480
13. Hou Q, Ge P, Lu G, et al. (2022) A novel PEMFC-CHP system for methanol reforming as fuel purified by hydrogen permeation alloy membrane. *Case Stud Therm Eng* 36: 102176. https://doi.org/10.1016/j.csite.2022.102176
14. Ma T, Jing G, Hu C, et al. (2025) Research on the mechanisms of contact resistance and structural deformation impact on PEMFC performance. *Case Stud Therm Eng* 74: 106845. https://doi.org/10.1016/j.csite.2025.106845
15. Owejan JP, Gagliardo JJ, Sergi JM, et al. (2009) Water management studies in PEM fuel cells, Part I: Fuel cell design and in situ water distributions. *Int J Hydrogen Energy* 34: 3436–3444. https://doi.org/10.1016/j.ijhydene.2008.12.100
16. Wang Z, Liao P, Long F, et al. (2025) Maritime electrification pathways for sustainable shipping: Technological advances, environmental drivers, challenges, and prospects. *eTransportation* 26: 100462. https://doi.org/10.1016/j.etran.2025.100462
17. Windarto C, Setiawan A, Duy NHX, et al. (2023) Investigation of propane direct injection performance in a rapid compression and expansion machine: Pathways to diesel marine engine efficiency parity with spark discharge duration strategies. *Int J Hydrogen Energy* 48: 33960–33980. https://doi.org/10.1016/j.ijhydene.2023.05.131
18. Yandem G, Willner J, Jabłońska-Czapla M (2025) Integrating photovoltaic technologies in smart cities: Benefits, risks and environmental impacts with a focus on future prospects in Poland. *Energy Rep* 13: 2697–2710. https://doi.org/10.1016/j.egyr.2025.02.014
19. Singla MK, Muhammed Ali SA, Gupta J, et al. (2025) Seven-parameter PEMFC model optimization using an battlefield optimization algorithm. *Electrochem Commun* 179: 108033. https://doi.org/10.1016/j.elecom.2025.108033

20. Xu Y, Zhang Y, Zheng J, et al. (2025) Effects of channel-land configuration on temperature-driven water transport in cathode gas diffusion layer of PEMFC. *Case Stud Therm Eng* 65: 105601. https://doi.org/10.1016/j.csite.2024.105601
21. Yang J, Chen L, Wu X, et al. (2025) Remaining useful life prediction of vehicle-oriented PEMFCs based on seasonal trends and hybrid data-driven models under real-world traffic conditions. *Renewable Energy* 249: 123193. https://doi.org/10.1016/j.renene.2025.123193
22. Rao CK, Sahoo V, Yanine FF (2024) A literature review on an IoT-based intelligent smart energy management systems for PV power generation. *Hybrid Adv* 5: 100136. https://doi.org/10.1016/j.hybadv.2023.100136
23. Robalo-Cabrera I, Alcayde A, Filgueira-Vizoso A, et al. (2025) Shipping sector decarbonisation measures: A review. *Sustainable Energy Technol Assess* 82: 104549. https://doi.org/10.1016/j.seta.2025.104549
24. Sarath S, Vijayakumar K (2025) High-gain MSHS converter with TCH-DAG controlling model for smart PV-EV charging systems. *J Energy Storage* 134: 118318. https://doi.org/10.1016/j.est.2025.118318
25. Alrwashdeh SS, Alsaraireh FM, Saraireh MA, et al. (2018) In-situ investigation of water distribution in polymer electrolyte membrane fuel cells using high-resolution neutron tomography with 6.5 μm pixel size. *AIMS Energy* 6: 607–614. https://doi.org/10.3934/energy.2018.4.607
26. Karakaya, C., Huang J, Cadigan C, et al. (2022) Development, characterization, and modeling of a high-performance Ru/B2CA catalyst for ammonia synthesis. *Chem Eng Sci* 247: 116902. https://doi.org/10.1016/j.ces.2021.116902
27. Zhang M, Zhu T, Huo Z, et al. (2024) A study of the promotion mechanism of digital inclusive finance for the common prosperity of Chinese rural households. *Front Earth Sci*, 12. https://doi.org/10.3389/feart.2024.1301632
28. Ince UU, Markötter H, George MG, et al. (2018) Effects of compression on water distribution in gas diffusion layer materials of PEMFC in a point injection device by means of synchrotron X-ray imaging. *Int J Hydrogen Energy* 43: 391–406. https://doi.org/10.1016/j.ijhydene.2017.11.047
29. Xu C, Chen Q, Liu S, et al. (2026) Study on optimization control of thermal management system for lithium-ion battery pack. *Appl Therm Eng* 282: 128800. https://doi.org/10.1016/j.applthermaleng.2025.128800
30. O'Hayre R, Haile SM (2025) Solid-state hydrogen storage goes electric Electrochemistry enables reversible storage and release of hydrogen gas in a metal hydride. *Science* 389: 1187–1188. https://doi.org/10.1126/science.aeb3327
31. Zhang Z, Zhou H, Wang G, et al. (2025) Chlorine evolution characteristics during lab-scale combustion of MSW pyrolysis char obtained from 200 t/d pyrolysis demonstration plant. *Waste Manage* 203: 114882. https://doi.org/10.1016/j.wasman.2025.114882
32. Xu, S., Murugesan TM, Elfar AAA, et al. (2024) Evaluation of sustainable manufacturing performance—A case illustration with multistakeholder perspective. *J Cleaner Prod* 458: 142368. https://doi.org/10.1016/j.jclepro.2024.142368
33. Alrwashdeh SS, Markötter H, Haußmann J, et al. (2016) Investigation of water transport dynamics in polymer electrolyte membrane fuel cells based on high porous micro porous layers. *Energy* 102: 161–165. https://doi.org/10.1016/j.energy.2016.02.075
34. Alrwashdeh SS, Markötter H, Haußmann J, et al. (2016) *X-ray tomographic investigation of water distribution in polymer electrolyte membrane fuel cells with different gas diffusion media*. *ECS Trans,* 72. https://doi.org/10.1149/07208.0099ecst

35. Pan Z, Wang J, Zhu L, et al. (2025) Performance and stability of renewable fuel production via H_2O electrolysis and H_2O–CO_2 co-electrolysis using proton-conducting solid oxide electrolysis cells. *Appl Energy* 385: 125571. https://doi.org/10.1016/j.apenergy.2025.125571
36. Shahgaldi S, Alaefour I, Unsworth G, et al. (2017) Development of a low temperature decal transfer method for the fabrication of proton exchange membrane fuel cells. *Int J Hydrogen Energy* 42: 11813–11822. https://doi.org/10.1016/j.ijhydene.2017.02.127
37. Al-Falahat AM, Kardjilov N, Khanh TV, et al. (2019) Energy-selective neutron imaging by exploiting wavelength gradients of double crystal monochromators—Simulations and experiments. *Nucl Instrum Methods Phys Res, Sect* 943: 162477. https://doi.org/10.1016/j.nima.2019.162477
38. Alrwashdeh SS (2018) Comparison among solar panel arrays production with a different operating temperatures in Amman-Jordan. *Int J Mech Eng Technol* 9: 420–429. Available from: https://iaeme.com/MasterAdmin/Journal_uploads/IJMET/VOLUME_9_ISSUE_6/IJMET_09_06_047.pdf.

AIMS Press